PHASE SPACE TOMOGRAPHY USING THE CORNELL ERL DC GUN

F.E. Hannon, Thomas Jefferson National Accelerator Facility, Newport News VA*
I.V. Bazarov, B. Dunham, Y. Li, X. Liu, Cornell University, Ithaca, NY

Abstract

The brightness and quality of electron beams in linac-based light sources are ultimately limited by the properties of the beam in the injector. It is thus important to have knowledge of the phase space distribution in addition to the rms emittance to provide an insight into high beam brightness formation mechanisms. A tomography technique has been used to reconstruct the transverse phase space of the electron beam delivered from the Cornell University ERL DC gun. The tomography diagnostic utilised three solenoid magnets directly after the DC gun and a view-screen. The injector was operated at 250keV in the emittance dominated regime, and the results showed good agreement to the phase space measured using a slit-screen method and that generated from simulation with the particle tracking code ASTRA. Comparison of various reconstruction methods is provided.

INTRODUCTION

Tomography

Tomography is used as a technique to reconstruct images to higher dimensionality from sets of profiles. It is most commonly known from the medical physics arena. The first experiments utilised x-rays to form a 3D model of tissue from a set of its 2D x-ray absorption images taken at different angles. The process of inferring information from density distributions that cannot be measured directly is ideal for use with electron beams where distributions of phase space are indirectly accessible.

Tomography is based on a theorem by Radon, who has shown that an object can be completely reconstructed from an infinite set of all its projections. In practice, it is not possible to collect an infinite number of projections, and so some error is introduced when the reconstruction is performed. The aim is to reduce this error through the correct choice of reconstruction algorithm for the problem.

A projection can be calculated by integrating some distribution, $f(x,y)$, along a line. The equation of a line and its integral is:

$$x\cos\theta + y\sin\theta = t\,,\ P_\theta(t) = \int_{\theta,t} f(x,y)ds \qquad (1)$$

The projection, or Radon transform, of $f(x,y)$ expanded using the delta function is given below, and forms the basis of tomography reconstruction procedures.

$$P_\theta(t) = \iint f(x,y)\delta(x\cos\theta + y\sin\theta - t)dxdy \quad (2)$$

There have been many methods employed previously in phase space reconstruction experiments. A list of tomography experiments can be found in [1,2]. Excluding the multi-turn tomography measurements in synchrotrons, where Gaussian approximations are made, all have used quadrupoles to rotate the phase space. Some experiments use a well known repeating lattice of quadrupoles, where the phase rotation between each cell is defined. Profile measurement devices are placed in each cell and used for reconstruction [2]. A disadvantage of this method is that only a few projections can be taken, and this limits the choice of reconstruction algorithm used. Using the Cornell ERL DC gun and a diagnostic beamline this technique was extended to consider solenoids as the elements used for rotating the phase space.

For a charged particle beam, the aim is to determine the transverse 2D phase space distribution, $\mu(x_0, x'_0)$ at some location z_0 along the beamline. If $\mu(x_1, x'_1)$ is the phase space distribution at z_1 and the system is linear, the phase space at z_1 can be calculated using the transfer matrix $\boldsymbol{R}$:

$$\begin{pmatrix} x_1 \\ x'_1 \end{pmatrix} = \boldsymbol{R}\begin{pmatrix} x_0 \\ x'_0 \end{pmatrix},\ \boldsymbol{R} = \begin{pmatrix} R_{11} & R_{12} \\ R_{21} & R_{22} \end{pmatrix} \qquad (3)$$

Following [1], a projection of the phase space at angle θ in the form of the Radon transform is given by:

$$P(x)s = \iint \mu(x_0, x'_0)\,\delta(cos\theta x_0 + sin\theta x'_0 - u)dx_0dx'_0$$
$$u = x/\sqrt{{R_{11}}^2 + {R_{12}}^2} \qquad (4)$$

This shows a simple relationship between the projection and the Radon transform, equation 1. The x coordinate of the measured profile is scaled with $1/s$ and the projection with s ($s=\sqrt{{R_{11}}^2+{R_{12}}^2}$). The rotation of phase space is $\tan\theta = R_{12}/R_{11}$. These equations form the basis of the quadrupole scan method, where the matrix is varied by changing the strength of quadrupoles between z_0 and z_1. The matrix elements are used to calculate the rotation and scaling. Two or more quadrupoles are needed to achieve rotation over a full 180°. As quadrupoles are focusing in one plane whilst simultaneously defocusing in the other, different settings are required to recreate the horizontal and vertical phase space. The advantage of using solenoids is that both transverse planes can be reconstructed from the same set of measurements.

Unlike quadrupoles, there is coupling between the x and y planes with solenoids due to the rotation. However any 4x4 transfer matrix can be expressed as the product of two affine matrix operations: scaling and rotation. The solenoid 4x4 transfer matrix can therefore be written as a product of decoupled thick lens $\mathbf{R_{dec}}$ and rotation matrices $\mathbf{R_{rot}}(KL)$:

$$R_{sol} = \begin{pmatrix} C & S/K & 0 & 0 \\ -KS & C & 0 & 0 \\ 0 & 0 & C & S/K \\ 0 & 0 & -KS & C \end{pmatrix}\begin{pmatrix} C & 0 & S & 0 \\ 0 & C & 0 & S \\ -S & 0 & C & 0 \\ 0 & -S & 0 & C \end{pmatrix}$$

* Authored by Jefferson Science Associates, LLC under U.S. DOE Contract No. DE-AC05-06OR23177. The U.S. Government retains a non-exclusive, paid-up, irrevocable, world-wide license to publish or reproduce this manuscript for U.S. Government purposes.

C = cos(KL), S = sin(KL), with Larmor angle *KL*, where $K = B_z/(2B\rho)$ for a region of uniform axial magnetic field of magnitude B_z and length *L*. For a beamline consisting entirely of solenoids the 2x2 $\mathbf{R_{dec}}$ matrix is simply the product of the corresponding decoupled solenoid and drift matrix elements. Additionally, the total Larmor angle is calculated as $\theta_L = \int Bz/(2B\rho)$ dz. Both the $\mathbf{R_{dec}}$ and θ_L were calculated using a field map of the solenoids rather than a thin lens approximation for a significant increase in accuracy. Once the obtained *x,y* images are rotated by $-\theta_L$, the problem of tomography is reduced to the usual 2D phase space reconstruction with both *x,x'* and *y,y'* distributions available simultaneously.

Reconstruction Algorithms

The most common reconstruction algorithm used for tomography is the filtered back projection (FBP) algorithm, [1].It is widely used because the mathematics is simple and easily programmable. However, for a small number of projections, streaking artefacts dominate the reconstructed image.

Choosing the optimum algorithm to use is largely dependent on the problem being solved. Some algorithms are better at reconstructing Gaussian distributions, whilst others are suited to detailed distributions. Popular reconstruction algorithms used for phase space tomography, in addition to the FBP method, are the maximum entropy (MENT) algorithm, used at Los Alamos, DESY and Tokyo University [2,3,4], and the maximum likelihood - expectation maximization (MLEM), used at Kyoto University [5].

Iterative reconstruction methods start with an estimate of an object function, and establish a relation between that and the measured projections. Then a minimisation problem is formed to measure the distance between the model generated projections and those measured. The MLEM is one such iterative method [6]. The algorithm is designed to compute the most likely distribution, given the measured projections. An advantage of this method is that fewer projections are needed to reconstruct simple shapes. However, the time taken to make the reconstruction increases as more iterations are required.

CORNELL DC GUN BEAMLINE

Diagnostic Beamline Layout

For tomography to work well the beamline needs to have the flexibility to produce a set of matrices that will give a good range of rotations for the projections, ideally spaced equally between 0 and 180° to give all aspects of the distribution. In addition the scaling must give measurable beam sizes at the measurement position.

The beamline, shown in figure 1, was therefore designed to perform under these constraints. The photo-cathode, which is located inside a DC gun (not shown) is situated on the right of the schematic. A set of corrector magnets align the electron trajectory through the centre of three solenoids. The complete diagnostic suite consists of 4 view screens, a wirescanner, a Faraday cup, a beam position monitor and 2 horizontal slits. The second view screen, after the solenoids, was used to collect the images for tomography using a 12-bit camera, and the slit diagnostic used for direct phase space measurements to compare with tomographically reconstructed distributions.

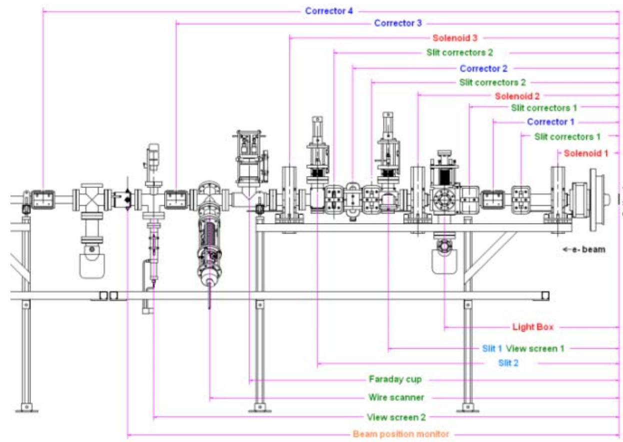

Figure 1: Beamline layout for tomography experiments.

Experiment

Solenoid settings were found to give 18 equally spaced rotations. The matrix element R_{12} was independently measured for a few cases using the first solenoid and view screen. The error between measurement and calculation increased with increasing solenoid peak field to a maximum of 7.5%. For each rotation the magnets were cycled to reduce hysteresis errors before being set. Image-grabbing software was used to select a region of interest around the beam spot on the screen and record the image. Each image was subject to a threshold to eliminate background noise, rotated by the Larmor angle and centred on the mean position. The projection along each axis was calculated by summing the pixels in that dimension. The projections were then scaled and used for reconstruction.

Two experiments were performed. The starting condition at the cathode for the first experiment was a 50MHz electron beam with a 2mm flat-top transverse and 30ps FWHM longitudinal distribution generated from a 520nm laser [7]. The electron gun was operated at 250kV and the beam current measured by the Faraday cup was <1μA. The negligible space charge in the beam implies that the measured emittance is entirely thermal, as measured in [8].

A second experiment was conducted using an electron beam that was split into two halves vertically. For this a 532nm laser was used to image a 2.6mm diameter aperture with a 0.6mm wire bisecting it onto the cathode.

RESULTS

The result of the reconstructed vertical phase space at 15cm from the cathode is shown in figure 2. 18 projections were used, with a threshold of 2%, and 70 iterations of the MLEM algorithm were performed. The normalised emittance calculated from the reconstruction is 0.258μm horizontally and 0.287μm vertically, within

6% and 18% respectively of the thermal emittance expected of 0.243 µm.

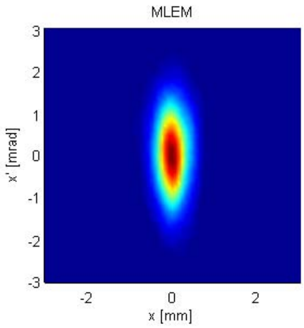

Figure 2: Reconstruction of phase space (single beam).

The error in this measurement may be attributed to jitter in the laser position causing non-symmetric beam images and non uniform background noise present on the view screens.

The result of the split beam experiment compared to simulation is shown in figure 3. A 1% threshold was applied to the images as the data set was rather clean. The two lobes are clearly visible in the reconstruction of the vertical plane and the horizontal reconstruction, although larger, shows the main features of phase space. The difference between the ASTRA [9] model and that measured is most likely due to difficulties in estimating the thermal emittance of an unusually shaped beam. The emittances calculated from the horizontal and vertical reconstruction are 0.448µm and 0.59µm respectively.

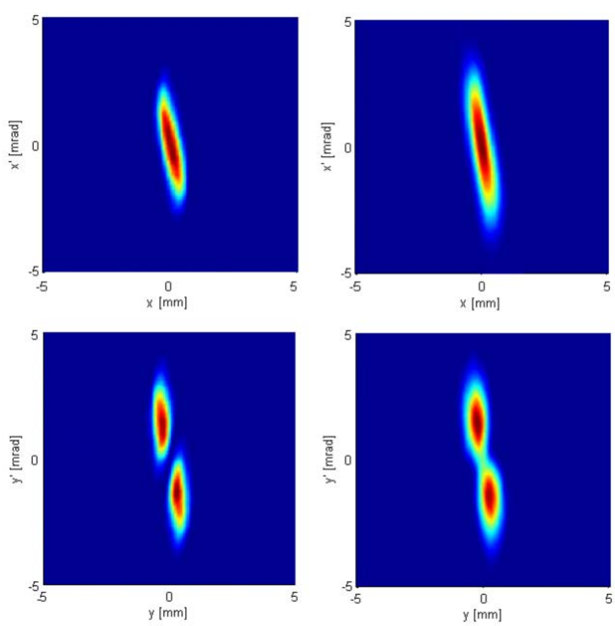

Figure 3: ASTRA (left) reconstructed (right) horizontal (top) and vertical (bottom) phase space.

To compare the vertical emittance, a double slit measurement was taken at 1.2m from the cathode, as described in [8]. This is shown in figure 4. Note: the different orientation of the phase space distribution is due to the double slit apparatus being positioned in a different location from the tomography reconstruction. The emittance calculated from the image (with 1.5% cut-off threshold) and using the SCUBEEx [10] technique gave 0.450µm and 0.445µm respectively. The difference between the direct phase space measurement and the reconstruction is 18%.

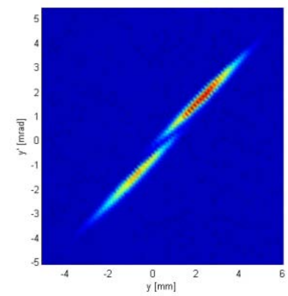

Figure 4: Phase space measured using a double slit.

CONCLUSIONS

Phase space tomography of emittance dominated beams will reconstruct the features of phase space that cannot be inferred from emittance measurements using the solenoid or quadrupole scan method, particularly for non Gaussian beams.

Solenoids can be successfully used as an alternative to quadrupoles for tomography experiments that produce the transverse phase space in both planes simultaneously. The reconstructions show the features of phase space well. We demonstrate that the method can be used to obtain qualitative information about the phase space (e.g. rms emittance), which was found in agreement to that measured by a direct method. However attention to the details of the reconstruction algorithm and image processing is required.

Finally, an attempt was made to apply tomography to space charge dominated bunched beam (~20 pC/bunch) employing a 50 MHz 520 nm laser [7]. The transfer matrix was augmented using linear space charge forces [1]. Results of the tomography reconstruction is this case were inconsistent, thought to be due to several factors such as: difficulty of obtaining sufficient rotation angles, and the fact that a simple linear space charge is insufficient to describe bunched beams with changing aspect ratio as found in the Cornell system.

REFERENCES

[1] D. Stratakis et al. *PRST-AB, 9*, 112801, 2006
[2] F. Loehl."Measurements of the Transverse Emittance at the VUV-FEL", DESY, Hamburg, 2005
[3] C.T. Mottershead et al. *PAC85*, p1970
[4] R. Hajima et al. *NIM-A*, 389:65–68, 1997
[5] H. Zen et al. *FEL06*, p668
[6] L.A. Shepp et al. *IEEE Trans Med Img*, MI1-2, 1982
[7] D.G. Ouzounov et al. *PAC07*, p530
[8] I.V. Bazarov et al. *J. App Phys,* 103, 054901 2007
[9] K. Floettmann. http://www.desy.de/˜mpyflo/... Astra_dokumentation/Manual_part1.pdf
[10] M.P. Stockli. Rev Sci Inst, 75-5, 2004